A PGSE NMR Approach to the Characterization of Single and Multi-Site Halogen-Bonded Adducts in Solution†

Gianluca Ciancaleoni,[a,*] Alceo Macchioni,[b] Luca Rocchigiani,[b,c] Cristiano Zuccaccia[b]

[a] *Departamento de Química, Universidade Federal de Santa Catarina, 88040-900 Florianópolis, SC,Brazil.*

[b] *Dipartimento di Chimica, Biologia e Biotecnologie, Universitá degli Studi di Perugia, Via Elce di Sotto 8, I-06123, Perugia,Italy*

[c] *School of Chemistry, University of East Anglia, Norwich, NR4 7TJ, UK*

*e-mail address: g.ciancaleoni@ufsc.br

† Electronic Supporting Information (ESI) available

Abstract. We demonstrate here that Pulsed field Gradient Spin Echo (PGSE) NMR diffusion technique can be effectively used as a complementary tool for the characterization of mono- and multi-site intermolecular halogen bonding (XB) in solution. The main advantage of this technique is that it provides the possibility of unambiguously determining the stoichiometry of the supramolecular adduct, an information that is particularly important when multi-site molecular systems are studied. As an example, PGSE NMR measurements in chloroform indicate that hexamethylenetetramine (**HMTA**), a potentially four-sites XB acceptor, actually exploits only two sites for the interaction with the XB donor N-bromosuccinimide (**NBS**), leaving the other two nitrogen sites unoccupied. Charge Displacement calculations suggest that this is due also to the anti-cooperativity of the XB interaction between **HMTA** and **NBS**.

Introduction

Halogen bonding (XB),[1] i.e. the non–covalent interaction between an halogen atom (XB donor) and a Lewis base (XB acceptor), mostly reveals its potential in solid state chemistry, being nowadays a powerful tool for the engineering of advanced materials[2,3,4] and a relevant motif in the structure of biomolecules.[5] XB emerged also as an interesting topic for theoretical chemistry, which tried to determine, not without controversies, the relative weights of charge transfer, electrostatic, dispersion, and polarization effects to XB.[6] In the last few years, XB started to find intriguing applications even in solution, mainly in catalysis[7] and anion recognition.[8] As a consequence, the characterization of the supramolecular structure of XB adducts in solution and the determination of the formation equilibrium constants have assumed a higher importance, also because the pattern of intermolecular interaction in solution could differ from that found at the solid state.

Recently, it has been suggested[9] that halogen bonding is not the only interaction that XB donors and acceptors can establish in solution, even when no other obvious interactions are possible, leading to adducts with different geometries but same stoichiometry. We recently demonstrated that ^{19}F, ^{1}H HOESY NMR, previously exploited with success to investigate ion pairing[10] and frustrated Lewis pairs,[11] can be also exploited to disclose the intermolecular structure of XB adducts.[12] Furthermore, in combination with theoretical studies, it can be used to estimate the relative weights of XB and non-XB interactions.[12]

Concerning the equilibrium constants involved in the XB interactions, many useful titration techniques have been applied[13,14] and the choice of the best one (UV-Vis, IR, NMR…) depends on the nature of the system under investigation. In all cases, the presence of more interactions is a potential complication, because the effect of each interaction on the experimental observable is, in principle, of a different magnitude, and their disentanglement is not easy. An additional layer of complexity arises when multi-site acceptors and donors are taken into account. In this case, the exact nuclearity of the adduct should be known *a priori*, since the fitting equation depends on the stoichiometry of the adduct (except when the different aggregation steps are clearly consecutive and

with very different affinities).[14] Information about the latter can be derived from the Job´s plot, but the general applicability of this technique is limited[15] and its coupling with other methodologies is always desirable.

Here, we propose the diffusion Pulsed field Gradient Spin Echo (PGSE)[16,17] NMR technique as a tool for the characterization of mono- and multi-site intermolecular halogen bonding systems, with the only requirement that NMR-active nuclei (preferably ^{1}H, ^{19}F or ^{31}P) are present on at least one, but preferably both, of the components. To the best of our knowledge, such a technique has been applied only in two recent cases, to support the formation of strong halogen-bonded adducts and to study the counterion influence on the same adduct.[18,19]

PGSE NMR allows information about the hydrodynamic volume (V_H) of molecular species in solution to be determined.[17] In the case of an aggregation process, the measured V_H increases, allowing the estimation of the equilibrium constants (K_a) involved in the process.[20] Remarkably, in the case of 1:1 adducts, the K_a can be evaluated by one single experiment,[21] making it a useful tool for preliminary measurements.

Furthermore, since PGSE NMR is based exclusively on the V_H, it takes into account all the possible aggregation processes, irrespectively from the supramolecular structure of the adduct. This offers the possibility to validate the data coming from titration techniques, where the effect of various interactions could be different on the chosen observable, with the general rule that K_a (PGSE) $\geq K_a$ (titration). In addition, PGSE NMR is very useful when investigating symmetric multi-site XB donors or acceptors, since it gives directly the average size of the adducts and allows the determination of the average number of units that are interacting.

To illustrate the potential of the PGSE approach, we considered here Lewis acids and bases shown in Scheme 1, which already proved to be XB acceptors/donors,[22] having different XB strength and number of sites. In particular, 1,4-diazabicyclo[2.2.2]octane (**DABCO**) and hexamethylenetetramine (**HMTA**) are commonly used in the fabrication of crystalline materials assembled by XB.[23]
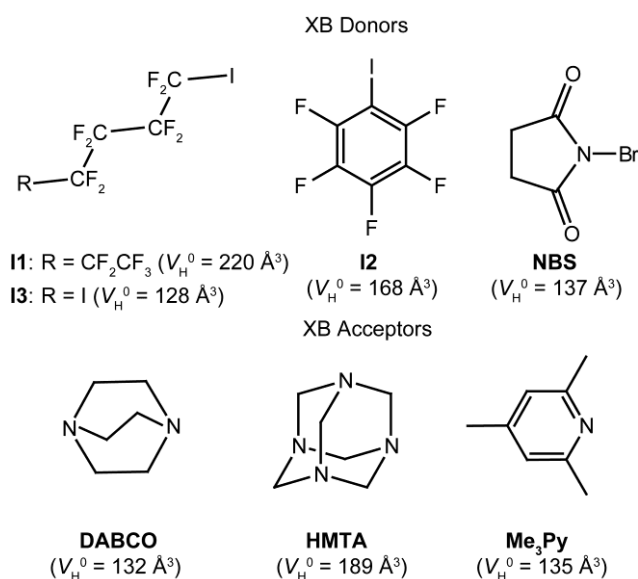
Scheme 1. XB donors and acceptors considered in this work. In parenthesis, the respective values for the hydrodynamic volume of the single molecule (V_H^0) are reported.

In both cases, the number of nitrogen atoms involved in XB interactions depends on the XB donor and the crystallization conditions. 2,4,6-Trimethylpyridine (**Me₃Py**) is rarely used because the resulting XB adduct is very weak, so weak that other minor interactions, as lone pair/π, cannot be neglected.[12] On the other hand, perfluorinated alkanes and benzenes (as perfluorohexyl-1-iodide, **I1**, pentafluoroiodobenzene, **I2** and 2,4-diiodooctafluorobutane, **I3**) have always been used in XB studies,[24] whereas N-bromosuccinimide (**NBS**) only recently revealed its potential as XB donor.[22c]

Results and discussion

The quantification of the hetero intermolecular aggregation by PGSE NMR asks for the preliminary evaluation of the hydrodynamic volume of the single molecule (V_H^0) and their tendency to undergo self-aggregation.

For this reason, we initially performed PGSE NMR experiments on solutions of increasing concentration of the single components in toluene-d_8 or chloroform-d, obtaining concentration-independent (within the experimental error of ±10%) values of V_H^0 equal to 220, 168, 128, 137,

135, 132 and 189 Å^3 for **I1**, **I2**, **I3**, **NBS**, **Me₃Py**, **DABCO** and **HMTA**, respectively (Table 1 and Scheme 1).

Table 1. Diffusion coefficients (D_t, 10^{-10} m^2 s^{-1}), hydrodynamic radii (r_H, Å) and hydrodynamic volumes (V_H, Å^3) of pure **Me₃Py**, **DABCO**, **I1** and **I2** measured in toluene-d_8 and **I3**, **HMTA** and **NBS** in chloroform-d at different concentrations (C, mM).

C	D_t	r_H	V_H
Me₃Py			
3.1	16.1	3.18	135
38.0	15.9	3.20	137
175	16.2	3.18	135
385	16.1	3.18	135
DABCO			
46.0	16.9	3.17	133
262	17.2	3.14	130
I1			
11.0	12.8	3.78	226
123	12.9	3.70	212
181	12.8	3.75	221
I2			
17.4	15.3	3.37	160
471	14.5	3.47	175
I3			
19.0	14.1	3.11	126
210.0	14.2	3.14	130

HMTA			
19.0	12.0	3.54	187
110	12.2	3.58	192
NBS			
5.4	14.3	3.20	137
61.0	14.3	3.20	137

The hydrodynamic volume of any adduct can be calculated by the sum of the V_H^0 values of the constituents (Eq. 1), always under the spherical approximation.[17]

$$V_H^{agg}(n\mathbf{D}, m\mathbf{A}) = n*V_H^0(\mathbf{D}) + m*V_H^0(\mathbf{A}) \qquad \text{Eq. 1}$$

Me₃Py/I1. As stated in the Introduction, substituted pyridines usually afford quite weak XB interactions. As a confirmation, for an equimolar mixture of **Me₃Py** and **I1**, the experimental hydrodynamic volumes of the two components ($V_H(\mathbf{Me_3Py})$ and $V_H(\mathbf{I1})$) are practically identical to the corresponding values of V_H^0 (Table 2). For this reason, only when a large excess of one of the components is used the measured V_H of the other component is significantly altered (Table 2). In particular, **I1**:**Me₃Py** molar ratios 1:3 or 1:14 are still not enough to have $V_H(\mathbf{I1})$ markedly different from its V_H^0, but using a molar ratio around to 1:200 leads to an increase of $V_H(\mathbf{I1})$ from 220 to 340 Å³ ($V_H^{agg}(\mathbf{Me_3Py}, \mathbf{I1}) = 355$ Å³). Being **Me₃Py** in large excess, $V_H(\mathbf{Me_3Py})$ is clearly close to its V_H^0, since most of the molecules are not involved in the formation of aggregates. By applying equations S1 and S2 (Supporting Information) to the experimental data with the lowest **I1**:**Me₃Py** molar ratio (Table 2), a value of $K_a = 1.6 \pm 0.5$ M⁻¹ is obtained.

Table 2. Diffusion coefficients (D_t, 10^{-10} m² s⁻¹) and hydrodynamic volumes (V_H, Å³) of **Me₃Py** / **I1** mixtures in toluene-d_8 at different concentrations (C, mM). In all the cases, $C(\mathbf{I1}) = 24$ mM.

$C(\textbf{Me}_3\textbf{Py})$	$D_t(\textbf{Me}_3\textbf{Py})$	$D_t(\textbf{I1})$	$V_H(\textbf{Me}_3\textbf{Py})$	$V_H(\textbf{I1})$
24.9	16.1	12.9	146	219
64.1	16.1	12.8	144	221
346	16.1	12.4	146	232
4910	15.7	10.3	152	340

On the other hand, the ^{19}F NMR titration method gives a value of $K_a = 0.85 \pm 0.01$ M[-1] (Figure S1, Supporting Information).[25] The titration allows to rapidly collect a large number of data, minimizing the experimental error. By the way, the formation constant obtained by diffusion measurements is double with respect to that obtained by the titration method, and this can be explained with the presence of two different 1:1 adducts, as already evidenced by HOESY results:[12] the observable of the titration (δ_F of the α fluorine atoms, -CF$_2$I) is mainly influenced by the XB interaction established between the nitrogen of **Me$_3$Py** and the iodine of **I1**, whereas the observable of the PGSE (V_H) is influenced by all the possible interactions, including electrostatic H$\cdots$F ones.[12] Since the K_a estimated by the PGSE measurement is the sum of all the equilibrium constants active in solution, by coupling the two techniques we can conclude that the formation constant of non-XB adducts is approximately 0.75 M^{-1}.

Remarkably, also combining ^{19}F, ^{1}H HOESY results with DFT calculations, the XB adducts resulted to be predominant over the non-XB ones (XB:non-XB = 78:22);[12] considering the approximations used in that paper, a reasonably good agreement is obtained.

Interestingly, in the solid state only the XB can be detected,[26] demonstrating that the supramolecular behavior of a pair in solution can differ from the structure of the same pair in the crystal.

DABCO/I1. In the case of multi-site XB acceptor, as **DABCO** is, the possibility of the 1:2 adduct must be taken into account. The symmetry of **DABCO** and the kinetic lability of XB in solution, hinder the possibility to use Overhauser-based experiments to determine how many nitrogen atoms

are interacting with the Lewis acid. Also in this case, the investigation of non-stoichiometric mixtures is very informative. In fact, studying the pair **DABCO/I1** in the presence of an excess of **DABCO** makes the concentration of the 1:2 adduct negligible and the analysis of $V_H(\textbf{I1})$ trends is related only to the formation of the 1:1 adduct (K_{a1}). On the other side, information about K_{a2} can be derived using an excess of **I1**.

Table 3. Diffusion coefficients (D_t, 10^{-10} m^2 s^{-1}) and hydrodynamic volumes (V_H, Å^3) of **DABCO** / **I1** mixtures in toluene-d_8 at different concentrations (C, mM).

$C(\textbf{DABCO})$	$C(\textbf{I1})$	$D_t(\textbf{DABCO})$	$D_t(\textbf{I1})$	$V_H(\textbf{DABCO})$	$V_H(\textbf{I1})$
3.6	20.0	12.8	12.3	221	239
17.6	20.0	13.7	11.9	194	250
108	20.0	15.1	10.3	162	328
7.0	37.0	12.0	–	250	–
7.0	85.0	10.5	–	326	–
7.0	216	9.2	–	426	–
7.0	343	8.5	–	517	–

Maintaining $C(\textbf{I1})$ constant at 20 mM (solvent: toluene-d_8) and increasing $C(\textbf{DABCO})$ from 3.6 to 108 mM, $V_H(\textbf{I1})$ increases from 239 to 338 Å^3, whereas $V_H(\textbf{DABCO})$ decreases from 221 to 162 Å^3. As stated before, the effect of aggregation is more visible on the least abundant species, consequently when $C(\textbf{DABCO}){<}C(\textbf{I1})$, $V_H(\textbf{I1})$ is just slightly larger than $V_H^0(\textbf{I1})$ and $V_H(\textbf{DABCO})$ is markedly larger than $V_H^0(\textbf{DABCO})$. On the contrary, when $C(\textbf{DABCO}){>}C(\textbf{I1})$, the situation is the opposite, with $V_H(\textbf{DABCO})$ similar to $V_H^0(\textbf{DABCO})$ and $V_H(\textbf{I1})$ markedly higher than $V_H^0(\textbf{I1})$. Indeed, when the concentration ratio **I1**:**DABCO** is 20:108, $V_H^0(\textbf{I1})$ approaches $V_H^{agg}(\textbf{DABCO}, \textbf{I1})$, which is 352 Å^3, evidencing an almost complete association of **I1** under these conditions.

Applying Eq. S1 and S2 (Supporting Information) to this single data, K_{a1} was estimated to be $34 \pm 10 \text{ M}^{-1}$, which corresponds to a free energy of association (ΔG_{a1}) of -2.1 kcal/mol. The ^{19}F NMR titration gives $K_{a1} = 37.2 \pm 0.4 \text{ M}^{-1}$ (Figure S2, Supporting Information), in agreement within the experimental errors.[27] In line with these findings, ^{19}F, ^{1}H HOESY NMR data demonstrated that non-XB interactions can be neglected for this particular pair.[12] Obviously, this does not mean that non-XB interactions are absent, but simply that their effects are completely hidden by the much more intense XB interaction, as in the PGSE as in the HOESY NMR experiments.

Successively, maintaining $C(\textbf{DABCO})$ at 7 mM and increasing $C(\textbf{I1})$ from 37 to 343 mM, $V_H(\textbf{DABCO})$ increases from 250 to 517 Å^3 (Table 3). In the last case, the hydrodynamic volume is much higher than $V_H^0(\textbf{DABCO})$, even higher than the volume of the 1:1 adduct (352 Å^3) and close to that of the 1:2 adduct ($V_H^{agg}(\textbf{DABCO}, 2\textbf{I1}) = 572 \text{ Å}^3$).

The data of $V_H(\textbf{DABCO})$ as a function of $C(\textbf{I1})$ can be fitted considering two equilibria (Figure 1 and equations S3 and S4, Supporting Information),[15] either imposing $K_{a1} = 34 \text{ M}^{-1}$, as determined previously, to find the best value of K_{a2} or optimizing both K_{a1} and K_{a2}. In the former case, $K_{a2} = 5 \pm 1 \text{ M}^{-1}$ ($\Delta G_{a2} = -0.9$ kcal/mol); in the latter case, $K_{a1} = 17 \pm 6 \text{ M}^{-1}$ and $K_{a2} = 7 \pm 2 \text{ M}^{-1}$. The results of the two methodologies are qualitatively similar, even if the second one, having more degrees of freedom, better fits the experimental data (Figure 1). In any case, K_{a2} is lower than K_{a1}. This is likely due to the low entropy of the adduct formed by three molecules.
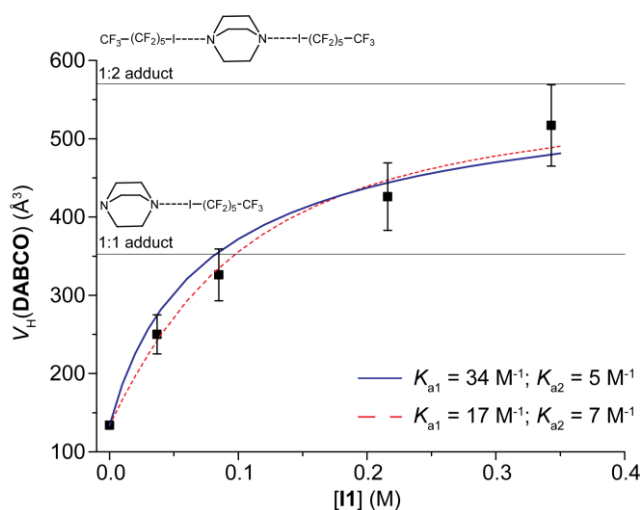
Figure 1. Experimental hydrodynamic volume of **DABCO** (C = 7 mM) at different concentrations of **I1**. The two lines represent the best fits obtained keeping K_{a1} constant (solid blue line) or not (dashed red line). See text for the details.

More importantly, the PGSE results offer an immediate and intuitive insight into the nuclearity of the adducts, at each concentration ratio (Figure 1).

DABCO/I2. Three solutions of **DABCO** (8.8 mM) in toluene-d_8 with increasing concentrations of **I2** (44, 177 and 403 mM) have been studied (Table 4). Under these experimental conditions, V_H(**DABCO**) spans from 194 to 352 Å^3, reaching a value that is in between V_H^{agg}(**DABCO**, **I2**) and V_H^{agg}(**DABCO**, 2**I2**). The fitting of the data, using V_H^{agg}(**DABCO**, **I2**) = 303 Å^3 and V_H^{agg}(**DABCO**, 2**I2**) = 471 Å^3, leads to the values of 11.0 ± 0.2 and 2.1 ± 0.1 M^{-1} for K_{a1} and K_{a2}, respectively (ΔG_{a1} = -1.5 kcal/mol; ΔG_{a2} = -0.4 kcal/mol, Figure S3, Supporting Information).

Table 4. Diffusion coefficients (D_t, 10^{-10} m^2 s^{-1}) and hydrodynamic volumes (V_H, Å^3) of **DABCO** / **I2** mixtures in toluene-d_8 at different concentrations (C, mM).

C(**DABCO**)	C(**I2**)	D_t(**DABCO**)	V_H(**DABCO**)
8.8	44.0	13.6	194
8.8	177	11.2	286
8.8	403	10.1	352

HMTA/NBS. Crystallographic studies on the pairs **HMTA/NIS** (**NIS** = N-iodo-succinimide) and **HMTA/NBS** revealed many interesting properties of such systems.[22c] For example, in the former case all the four basic sites of **HMTA** interact with a molecule of **NIS**, while in the latter case only two nitrogen atoms interact with a molecule of **NBS**. Unfortunately, the solubility of the pair

HMTA/**NIS** is not enough to allow a PGSE NMR study, but the pair **HMTA**/**NBS** is soluble enough in chloroform-d, even if very large excesses of one component cannot be explored.

For **HMTA**/**NBS**, the calculated hydrodynamic volumes for the 1:1, 1:2, 1:3 and 1:4 adducts are 323, 457, 591 and 729 $\mathring{A}^3$, respectively.

Table 5. Diffusion coefficients (D_t, 10^{-10} m^2 s^{-1}) and hydrodynamic volumes (V_H, $\mathring{A}^3$) of **HMTA** / **NBS** mixtures in chloroform-d at different concentrations (C, mM).

C(**HMTA**)	C(**NBS**)	D_t(**HMTA**)	D_t(**NBS**)	V_H(**HMTA**)	V_H(**NBS**)
12.1	3.9	11.5	10.0	194	254
50.0	3.9	11.9	8.36	166	291
179	3.9	12.0	8.57	166	317
2.1	4.3	10.4	12.8	217	150
2.1	38.5	7.71	12.8	392	144
2.1	56.0	7.62	13.7	408	130
2.1	93.0[a]	7.45	13.7	438	131

[a] Saturated solution

Using chloroform-d as solvent and keeping C(**NBS**) fixed at 3.9 mM, three solutions with C(**HMTA**) = 12.1, 50 and 179 mM have been analyzed. V_H(**NBS**) increases as C(**HMTA**) increases, going from 254 to 317 $\mathring{A}^3$ (Table 5), which is very close to V_H^{agg}(**HMTA**, **NBS**). Fitting the data, K_{a1} results to be 161 ± 27 M^{-1} (Supporting Information).

In a second set of experiments, to a solution of **HMTA** (C = 2.1 mM) in chloroform-d, NBS was added to reach C(**NBS**) = 4.3, 38.5, 56 and 93 mM (Table 5). As before, the hydrodynamic volume of the component in excess decreases as its concentration increases (V_H(**NBS**) goes from 150 to 131 $\mathring{A}^3$), whereas the hydrodynamic volume of the other component (V_H(**HMTA**)) increases from 217 to 438 $\mathring{A}^3$. Noteworthy, passing from C(**NBS**) = 56 to 93 mM, V_H(**HMTA**) increases of only 30 $\mathring{A}^3$,

which is within the experimental error of 10%. Unfortunately, a higher concentration of **NBS** is not possible because of the solubility limit of the mixture, but the final value of V_H(**HMTA**) is very close to V_H^{agg}(**HMTA**, 2**NBS**). Such a value is the average of all the volumes of the species present in solution, but considering also that the trend of V_H(**HMTA**) *vs*. *C*(**NBS**) shows a *plateau* in the correspondence of V_H^{agg}(**HMTA**, 2**NBS**) (Figure 2), we can deduce that K_{a3} and K_{a4} are likely too small to be determined. Consequently, the experimental data can be fitted with the 1:2 model, in agreement with the crystal structure of this pair.[22c] The absence of a *plateau* in this range of V_{HS} (400-500 Å^3) would have been an indication for the existence of larger adducts, as 1:3 and 1:4. This reveals another great advantage of the diffusion NMR technique: for multi-site systems, the maximum stoichiometry is not a hypothesis, but can be derived from the trend of V_H with the concentration.
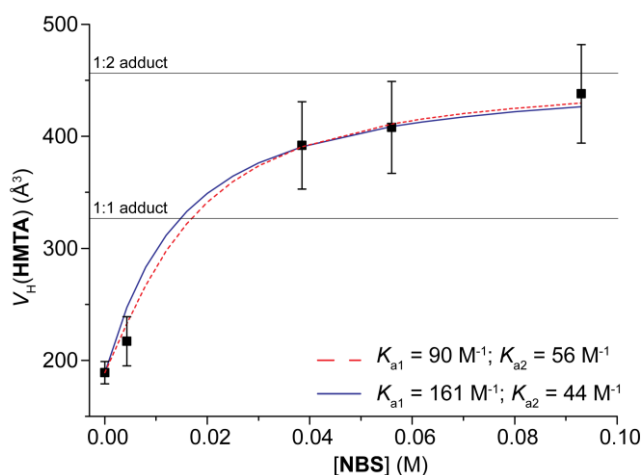

Figure 2. Experimental hydrodynamic volume of **HMTA** (*C* = 2.1 mM) at different concentrations of **NBS**. The two lines represent the best fits obtained keeping K_{a1} constant (solid blue line) or not (dashed red line). See text for the details.

Fitting the experimental data with the 1:2 model and fixing K_{a1} = 161, the best value of K_{a2} is 44 ± 12 M^{-1} (ΔG_{a2} = -2.2 kcal/mol), whereas optimizing both the values the results are 90 ± 20 and 56 ±

8 M^{-1}for K_{a1} and K_{a2}, respectively (ΔG_{a1} = -2.6 kcal/mol; ΔG_{a2} = -2.4 kcal/mol). Also in this case, both methodologies give similar results and, again, K_{a1} is larger than K_{a2}.

In order to understand better why the 1:3 adducts are not easily accessible in solution, DFT calculations have been performed on this system. Optimizing the structure of the 1:1, 1:2 and 1:3 adducts (level of theory M06-2X/def2-TZVP, as suggested by a recent, dedicated benchmark,[28] see details in the Computational Details), the N···Br distances results to be 2.533, 2.585 and 2.628 Å, respectively. The progressive lengthening of the N···Br distance already indicates that the interaction is weaker as the number of **NBS** molecules around the central **HMTA** increases.

Other information can be obtained with the Charge Displacement (CD) method,[29] which already proved to be useful for the characterization of coordinative[30] and non-covalent bonds,[11,31] including halogen bonding.[32] In particular, CD results demonstrated to be correlated linearly to the formation constants of chalcogen bonded adducts.[33]

In the case of 1:1 adducts, the difference of electron density ($\Delta\rho$) between the adduct and the separate fragments (**HMTA** and **NBS**) is shown in Figure 3a. It clearly shows that the nitrogen of **HMTA** is in a region of electron depletion, whereas a region of electron accumulation is present between the nitrogen and the bromine. As expected, a charge transfer between the two molecules exists, going from the nitrogen to the bromine. The latter shows a polarization pattern (depletion in the direction of **HMTA**, accumulation on the other side) and a remarkable region of electron accumulation is on the nitrogen of the **NBS**. The backbone of the **NBS** show a small charge accumulation, whereas the nitrogen atoms of the **HMTA** not involved in the XB show a small charge depletion, indication that the charge flux involve the entire system.
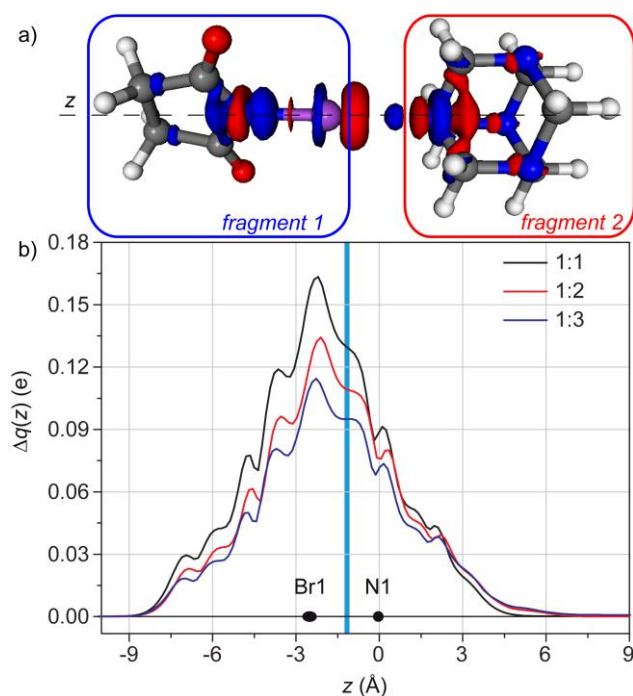
Figure 3. (a) 3D contour map of the change of electronic density upon formation of the adduct **HMTA**/**NBS** (1:1). Blue (red) isosurfaces identify regions in which the electron density increases (decreases). Density value at the isosurfaces: ±0.002 au. (b) Charge Displacement functions for **HMTA**/**NBS** adducts with different stoichiometry. The black dots represent the z coordinate (or the range of coordinates) of the atoms. The light blue vertical band identifies the range of the inter-fragment boundaries.

Integrating $\Delta\rho$ along the axis containing the nitrogen of **HMTA** and the bromine of **NBS** (z), the charge transfer (*CT*) can be quantified as 0.130 e (Figure 3b).

Applying the same method to the 1:2 and 1:3 adducts, the corresponding $\Delta\rho$ maps reveal a qualitative similarity with the one calculated for the 1:1 adduct (Figure 4a and Figure S5, Supporting Information). This is reasonable, since in all the cases the interaction is similar. From the quantitative point of view, the integration of the $\Delta\rho$ functions leads to *CT* values of 0.110 and 0.095 for the 1:2 and 1:3 adduct, respectively. The attenuation of the *CT* as the number of **NBS** molecules around the central **HMTA** increases gives a framework to explain the attenuation of the formation constants: the four nitrogen atoms on the **HMTA** are not mutually independent, and the

donation of electronic density from one nitrogen atom to a Lewis acid makes the donation properties of the non-involved nitrogen atoms lower.

This effect can be quantified applying the CD on a different axis.[34] If we consider the adduct between **HMTA** and two **NBS** moieties, we obviously have two interactions between two different nitrogen atoms of the **HMTA** and the two molecules of **NBS**. They can be labeled N1···**NBS1** and N2···**NBS2**. Taking as fragments **NBS1** and **HMTA/NBS2** and integrating $\Delta\rho$ along the axis containing N2 and the bromine of **NBS2** (Figure 4), the effect of the establishment of N1···**NBS1** on N2···**NBS2** can be evaluated. In this case, the analysis of the $\Delta\rho$ shows that, upon the formation of N1···**NBS1**, the nitrogen of **NBS2** is located in a region of electron density depletion. This indicates a charge transfer from **NBS2** to **HMTA**, leading to a XB weakening. The integration along the axis containing N2 and Br2 confirms the direction of the flux and leads to a weakening of 0.011 e (Figure 4b).
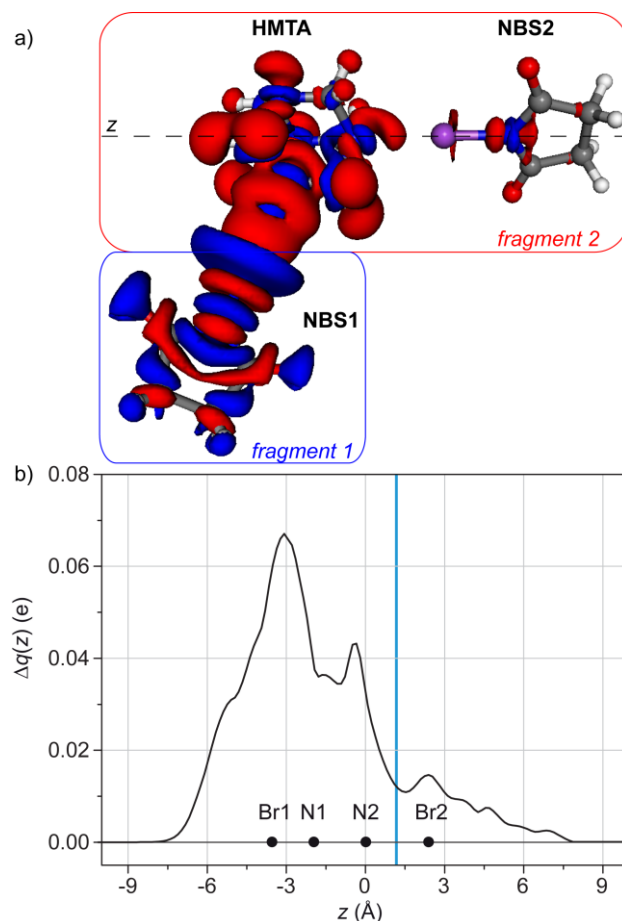
Figure 4. (a) 3D contour map of the change of electronic density upon formation of the adduct **HMTA**/**NBS** (1:2). Blue (red) isosurfaces identify regions in which the electron density increases (decreases). Density value at the isosurfaces: ±0.00025 au. (a) Charge Displacement functions for **HMTA**/**NBS**(1:2), integrated along the N2···Br2 axis. The black dots represent the z coordinate of the atoms. The light blue vertical band identifies the range of the inter-fragment boundaries.

The electronic energies ΔE of the 1:1, 1:2 and 1:3 adducts are -11.6, -20.5 and -28.0 kcal/mol (Supporting Information) with respect to the isolated components (see Table S1, Supporting Information). If we calculate $\Delta E/n$, where n is the number of **NBS** involved in the adduct, it results -11.6, -10.2 and -9.3 kcal/mol, respectively, again indicating that the interactions become weaker for larger aggregates (anti-cooperativity), in agreement with CD results. Therefore, the formation of adducts with higher stoichiometric ratios, as 1:3 and 1:4, is made difficult not only for obvious entropic reasons (each additional moiety loses its translational degree of freedom, making the ΔG more positive), but also for enthalpic ones (the charge transfer becomes weaker as the number of units increases). Interestingly, in other cases the XB resulted to be cooperative in nature.[35]

DABCO/I3. A very intriguing combination is when both the acceptor and the donor are multi-site, and, in principle, any n:m adduct can exist. The pair **DABCO/I3**, for example, is able to form infinite chains in the solid state.[36] Also in this case the pair presents a low solubility, limiting the possibility to use non-stoichiometric solutions. Anyway, at least three different situations can be explored: an excess of **DABCO**, an excess of **I3** and a substantial equivalence between the concentrations of the two components. In all the cases the solution is saturated, but both V_H(**DABCO**) and V_H(**I3**) are always much lower than 260 $Å^3$, which is the value of V_H^{agg}(**DABCO**, **I3**) (Table 6). Consequently, even if the presence of higher adducts cannot be excluded, their concentration should be very low in all cases.

Table 6. Diffusion coefficients (D_t, 10^{-10} m^2 s^{-1}) and hydrodynamic volumes (V_H, Å^3) of **DABCO** / **I3** mixtures in chloroform-d at different concentrations (C, mM).

C(**DABCO**)	C(**I3**)	D_t(**DABCO**)	D_t(**I3**)	V_H(**DABCO**)	V_H(**I3**)
85.8[a]	7.8	13.0	10.8	123	175
29[a]	21	12.6	11.8	159	180
16.7[a]	58	12.2	13.5	178	146

[a] Saturated solution

Applying Eq. S1 and S2 (Supporting Information) to the experiments where one component is in excess (C(**DABCO**) = 85.8 and C(**I3**) = 58 mM, Table 6), K_{a1} results to be 6 ± 2 and 10 ± 3 M^{-1}, respectively (ΔG_{a1} = -1.2 kcal/mol).

Conclusions

Diffusion NMR demonstrated to afford valuable information on the stoichiometry and the strength of the interactions of halogen-bonded adducts.

In particular, for the pair **Me₃Py/I1** the complementarity of the NMR titration and the PGSE method allowed the estimation of the formation constant of the adducts held together by interactions different from the XB (non-XB).

In the case of the ditopic halogen acceptor **DABCO,** both 1:1 and 1:2 adducts have been directly detected, either using aliphatic and aromatic perfluorinated XB donors (**I1** and **I2**). The corresponding formation constants have been evaluated and the formation of the 1:2 adduct showed an equilibrium constant considerably lower than that of the 1:1 adduct. For this system, the formation constant of the 1:1 adduct evaluated by NMR titration is in agreement with that measured by PGSE, indication that non-XB adducts are negligible.

The case of **HMTA** is even more interesting, since it bears four symmetric nitrogen atoms and all of them potentially could establish an interaction with **NBS**. PGSE NMR data unequivocally demonstrate that only two nitrogen atoms are involved in the interaction with **NBS** and, again, the formation constant of the 1:2 adduct resulted lower than that of the 1:1 adduct. DFT and Charge Displacement investigations demonstrated that each molecule of **NBS** that binds on a nitrogen atom of the **HMTA** reduces the electron-donating properties of the other nitrogen atoms (anti-cooperativity).

Finally, PGSE NMR data demonstrated also that the interaction between **DABCO** and **I3** is too weak in chloroform-*d* to produce aggregates larger than the 1:1 adduct, despite both the XB acceptor and donor possess two binding sites and despite the existence in the solid state of infinite chains.

In conclusion, PGSE NMR can be surely considered a powerful technique, which gives information that could be a complement for the titration methods routinely used up to now. For this reason, an integrated multi-technique approach, which include titrations, diffusion and Overhauser NMR techniques (but also DFT calculations, when needed) is highly desirable, for a complete characterization of XB systems in solution.

Experimental Section

All solvents and chemicals were purchased from Sigma–Aldrich and Cortecnet at the highest purity available and used as received. 1D and 2D NMR spectra were measured at 298 K on a Bruker DRX

Avance 400 spectrometer equipped with a BBFO probe, on a Bruker Avance III HD 400 spectrometer equipped with a smartprobe. Referencing is relative to residual of undeuterated solvents (^{1}H) and CCl$_3$F (^{19}F).

PGSE NMR Measurements. ^{1}H and ^{19}F PGSE NMR measurements were performed by using the double-stimulated echo sequence with longitudinal eddy current delay[37] at 298 K without spinning. The dependence of the resonance intensity (*I*) on a constant waiting time and on a varied gradient strength *G* is described by the following equation:

$$ln\frac{I}{I_0} = (\gamma\delta)^2 D_t \left(\Delta - \frac{\delta}{3}\right) G^2$$ Eq. 2

where *I* is the intensity of the observed spin echo, I_0 the intensity of the spin echo in the absence of gradient, D_t the self-diffusion coefficient, Δ the delay between the midpoints of the gradients, δ the length of the gradient pulse, and γ the magnetogyric ratio. The shape of the gradients was rectangular, their length δ was 4–5 ms, and their strength *G* was varied during the experiments. All spectra were acquired for 32k points and a spectral width of 5000 (^{1}H) and 18000 (^{19}F) and processed with a line broadening of 1.0. The semi-logarithmic plots of ln(I/I_0) versus G^2 were fitted by using a standard linear regression algorithm, and a correlation factor better than 0.99 was always obtained. Different values of Δ, *G*, and number of transients were used for different samples.

The self-diffusion coefficient D_t, which is directly proportional to the slope m of the regression line obtained by plotting ln(I/I_0) versus G^2, was estimated by evaluating the proportionality constant for a sample of HDO (5%) in D$_2$O (known diffusion coefficients in the range 274–318 K[38]) under the exact same conditions as the sample of interest. The solvent or TMS was taken as internal standard.

Computational Details. All the optimizations and thermodynamic calculations were performed using the Gaussian 09 program,[39] using density functional theory employinghybrid meta-generalized gradient approximation functional M06-2X[40]and the triple-ζ def2-TZVP basis set. The solvent and its polarity has been modeled through the PCM procedure (chloroform).[41] All the

optimized adducts show only positive vibrations, except **hmta-3nbs**, which showed three small uneliminable negative frequencies that could not be avoided during optimization. The negative vibrational modes were checked to make sure that they did not correspond to any motion along the halogen bond axes (bond formation or breaking). Rather, they refer to the rotation/vibration of the **NBS**s around the halogen bond axis.

All the Charge Displacement[29] calculations were carried out using density functional theory employing the same level of calculation used for optimizations. Such an approach relies on the integration along a given direction z (eq. 3) of the difference of electronic density $[\Delta\rho(x,y,z)]$ between the adduct and its non-interacting fragments, frozen in the same positions they occupy in the adduct.

$$\Delta q(z') = \int_{-\infty}^{\infty} dx \int_{-\infty}^{\infty} dy \int_{-\infty}^{z'} dz\, \Delta\rho(x,y,z) \qquad \text{Eq. 3}$$

The value of $\Delta q(z')$ defines the amount of the electronic charge that, upon formation of the adduct, has moved across a plane perpendicular to the axis through the coordinate z'. At the boundary between the fragments (the point on the z axis at which equal-valued isodensity surfaces of the isolated fragments are tangent) the value of Δq is represented by *CT*.

The electronic density matrices have been manipulated through the suite of tools "Cubes".[42]

References.

[1] G. R. Desiraju, P. S. Ho, L. Kloo, A. C. Legon, R. Marquardt, P. Metrangolo, P. Politzer, G. Resnati and K. Rissanen, *Pure Appl. Chem.*, 2013, **85**, 1711.

[2] (a) G. Berger, J. Soubhyea and F. Meyer, *Polym. Chem.*, 2015, **6**, 3559-3580; (b) L. C. Gilday, S. W. Robinson, T. A. Barendt, M. J. Langton, B. R. Mullaney and P. D. Beer, *Chem. Rev.*, 2015, **115**, 7118; (c) P. A. Gale and J. W. Steed, *Supramolecular Chemistry: from molecules to nanomaterials*,

John Wiley & Sons Ltd, New York, 1st edn, 2012; (d) G. Cavallo, P. Metrangolo, R. Milani, T. Pilati, A. Priimagi, G. Resnati and G. Terraneo, *Chem. Rev.*, 2016, **116**, 2478.

[3] (a) E. Corradi, S. V. Meille, M. T. Messina, P. Metrangolo and G. Resnati, *Angew. Chem. Int. Ed.*, 2000, **39**, 1782; (b) P. Metrangolo, H. Neukirch, T. Pilati and G. Resnati, *Acc. Chem. Res.*, 2005, **38**, 386; (c) P. Metrangolo, F. Meyer, T. Pilati, G. Resnati and G. Terraneo, *Angew. Chem., Int. Ed.*, 2008, **47**, 6114; (d) P. Metrangolo, Y. Carcenac, M. Lahtinen, T. Pilati, K. Rissanen, A. Vij and G. Resnati, *Science*, 2009, **323**, 1461.

[4] (a) F. Wang, N. Ma, Q. Chen, W. Wang and L. Wang, *Langmuir*, 2007, **23**, 9540; (b) H. L. Nguyen, P. N. Horton, M. B. Hursthouse, A. C. Legon and D. W. Bruce, *J. Am. Chem. Soc.*, 2004, **126**, 16; (c) O. Bolton, D. Lee, J. Jung and J. Kim, *Chem. Mater.*, 2014, **26**, 6644; (d) S.-Q. Zang, Y.-J. Fan, J.-B. Li, H.-W. Hou and T. C. W. Mak, *Cryst. Growth Des.*, 2011, **11**, 3395.

[5] (a) M. Carter, A. R. Voth, M. R. Scholfield, B. Rummel, L. C. Sowers and P. S. Ho, *Biochemistry*, 2013, **52**, 4891; (b) M. R. Scholfield, C. M. V. Zanden, M. Carter and P. S. Ho, *Protein Science*, 2013, **22**, 139; (c) P. Zhou, F. Tian, J. Zou and Z. Shang, *Mini-Reviews in Medicinal Chemistry*, 2010, **10**, 309.

[6] (a) L. P. Wolters, P. Schyman, M. J. Pavan, W. L. Jorgensen, F. M. Bickelhaupt and S. Kozuch, *WIREs Comput. Mol. Sci.*, 2014, **4**, 523; (b) S. Kozuch and J. M. L. Martin, *J. Chem. Theory Comput.*, 2013, **9**, 1918; (c) T. Clark, M. Hennemann, J. Murray and P. J. Politzer, *J. Mol. Model.*, 2007, **13**, 291; (d) P. Politzer, J. S. Murray and T. Clark, *Phys. Chem. Chem. Phys.*, 2010, **12**, 7748; (e) T. Clark, T. *WIREs Comput. Mol. Sci.* 2013, **3**, 13−20; (f) S. M. Huber, E. Jimenez-Izal, J. M. Ugaldeb and I. Infante, *Chem. Commun.*, 2012, **48**, 7708; (g) C. Wang, D. Danovich, Y. Mo and S. Shaik, *J. Chem. Theory Comput.* 2014, **10**, 3726.

[7] (a) A. Bruckmann, M. Pena and C. Bolm, *Synlett*, 2008,**2008**, 900; (b) S. M. Walter, F.Kniep, E.Herdtweck and S. M. Huber, *Angew. Chem. Int. Ed.*, 2011, **50**, 7187; (c) S.Dordonne, B.Crousse, D. Bonnet-Delpon and J.Legros, *Chem. Commun.*, 2011, **47**, 5855;(d) Lefèvre, G. Franc, C. Adamo, A. Jutand and I. Ciofini, *Organometallics* 2012, **31**, 914; (e) S. H. Jungbauer,S. M. Walter, S. Schindler, L. Rout, F.Kniepa and S. M. Huber, *Chem. Commun.*, 2014, **50**, 6281; (f) D. P. de Sousa, C.Wegeberg, M. S.Vad, S Mørup,C. Frandsen, W. A. Donald and Christine J. McKenzie, *Chem. Eur. J.* 2016, **22**, 3810; (g) V. P. N. Nziko and S. Scheiner, *J. Org. Chem.*, 2016, **81**, 2589.

[8] (a) M. J. Langton, I. Marques, S. W. Robinson, V. Félix and P. D. Beer, *Chem. Eur. J.*, 2016, **22**, 185; (b) S. W. Robinson, C. L. Mustoe, N. G. White, A. Brown, A. L. Thompson, P.Kennepohl and P. D. Beer, *J. Am. Chem. Soc.*, 2015, **137**, 499; (c) M. G. Sarwar, B. Dragisic, S. Sagoo and M. S. Taylor, *Angew. Chem. Int. Ed.*, 2010, **49**, 1674.

[9] (a) K. Gao and N. S. Goroff, *J. Am. Chem. Soc.*, 2000, **122**, 9320; P. D. Rege, O. L. Malkina and N. S. Goroff, *J. Am. Chem. Soc.*, 2002, **124**, 370; (b) N. Ma, Y. Zhang, B. Ji, A. Tian and W. Wang, *ChemPhysChem*, 2012, **13**, 1411.

[10] (a) G. Bellachioma, B. Binotti, G. Cardaci, C. Carfagna, A. Macchioni, S. Sabatini and C. Zuccaccia, *Inorg. Chim. Acta*, 2002, **330**, 44, (b) G. Ciancaleoni, L. Belpassi, F. Tarantelli, D. Zuccaccia and A. Macchioni, *Dalton Trans.*, 2013, **42**, 4122.

[11] L. Rocchigiani, G. Ciancaleoni, C. Zuccaccia and A. Macchioni, *J. Am. Chem. Soc.*, 2014, **136**, 112.

[12] G. Ciancaleoni, R. Bertani, L. Rocchigiani, P. Sgarbossa, C. Zuccaccia and A. Macchioni, *Chem. Eur. J.*, 2015, **21**, 440.

[13] M. Erdély, *Chem. Soc. Rev.*, 2012, **41**, 3547 and references within.

[14] S. H. Jungbauer, S. Schindler, E. Herdtweck, S. Keller and S. M. Huber, *Chem. Eur. J.*, 2015, **21**, 13625.

[15] P. Thordarson, *Chem. Soc. Rev.*, 2011, **40**, 1305.

[16] (a) G. Bellachioma, G. Ciancaleoni, C. Zuccaccia, D. Zuccaccia and A. Macchioni, *Coord. Chem. Rev.*, 2008, **252**, 2224; (b) P. S. Pregosin, *Spectroscopic Properties of Inorganic and Organometallic Compounds: Techniques, Materials and Applications,* 2011, **42**, 248; (c) L. Avram and Y. Cohen, *Chem. Soc. Rev.*, 2015, **44**, 586; (d) L. Rocchigiani and A. Macchioni, *Dalton Trans.*, 2016, **45**, 2785; (e) P. S. Pregosin, *Magn. Reson. Chem.* DOI: 10.1002/mrc.4394.

[17] A. Macchioni, G. Ciancaleoni, C. Zuccaccia and D. Zuccaccia, *Chem. Soc. Rev.*, 2008, **37**, 479.

[18] (a) A.-C. C. Carlsson, J. Gräfenstein, A. Budnjo, J. L. Laurila, J. Bergquist, A. Karim, R. Kleinmaier, U. Brath and M. Erdélyi, *J. Am. Chem. Soc.*, 2012, **134**, 5706; (b) M. Bedin, A. Karim, M. Reitti, A-C C. Carlsson, F. Topić, M. Cetina, F. Pan, V. Havel, F. Al-Ameri, V. Sindelar, K.Rissanen, J.Gräfenstein and M.Erdély, *Chem. Sci.*, 2015, **6**, 3746.

[19] During the evaluation process of the present paper, other two articles that use diffusional NMR techniques on XB systems have been published: (a) L. Maugeri, J. Asencio-Hernandez, T. Lébl, D. B. Cordes, A. M. Z. Slawin, M.-A. Delsuc and D. Philp, *Chem. Sci.*, DOI: 10.1039/c6sc01974a; (b) C. J. Massena, N. B. Wageling, D. A. Decato, E. M. Rodriguez, A. M. Rose and O. B. Berryman, *Angew. Chem. Int. Ed.*, DOI: 10.1002/anie.201605440.

[20] (a) L. Rocchigiani, G. Bellachioma, G. Ciancaleoni, S. Crocchianti, A. Laganá, C. Zuccaccia, D. Zuccaccia and A. Macchioni, *ChemPhysChem*, 2010, **11**, 3243; (b) G. Ciancaleoni, I. Di Maio, D. Zuccaccia and A. Macchioni, *Organometallics*, 2007, **26**, 489.

[21] L. Fielding, *Tetrahedron*, 2000, **56**, 6151.

[22] For **I1** and **DABCO**, see: (a) R. Cabot and C. A. Hunter, *Chem. Commun.*, 2009, 2005; for **I2**, see: (b) M. G. Sarwar, B. Dragisic, L. J. Salsberg, C. Gouliaras and M. S. Taylor, *J. Am. Chem. Soc.*, 2010, **132**, 1646; for **I3**, see ref 3d; for **NBS** and **hmta**, see: (c) K.Raatikainen and K.Rissanen, *CrystEngComm*, 2011, **13**, 6972; for **Me₃Py**, see: (d) C. Laurence, J. Graton, M. Berthelot and M. J. El Ghomari, *Chem. Eur. J.*, 2011, **17**, 10431.

[23] (a) R. B. Walsh, C. W. Padgett, P. Metrangolo, G.Resnati, T. W. Hanks and W. T. Pennington, *Cryst. Growth Des.*, 2001, **1**, 165; (b) C. Perkins, S. Libri, H. Adams and L. Brammer, *CrystEngComm*, 2012, **14**, 3033; (c) L. Catalano, S. Perez-Estrada, G. Terraneo, T. Pilati, G. Resnati, P. Metrangolo and M. A. Garcia-Garibay, *J. Am. Chem. Soc.*, 2015, **137**, 15386.

[24] E. Corradi, S. V. Meille, M. T. Messina, P. Metrangolo and G. Resnati, *Angew. Chem. Int. Ed.*, 2000, **39**, 1782.

[25] K_a for the pair **Py**/**I1** in benzene results to be 1.0, see ref. 22a.

[26] A. Wasilewska, M. Gdaniec and T Połoński, *CrystEngComm*, 2007, **9**, 203.

[27] K_a for the pair **DABCO**/**I1** in benzene results to be 32, see ref. 22a.

[28] S. Kozuch and J. M. L. Martin, *J.Chem. Theory Comput.*, 2013, **9**, 1918.

[29] L. Belpassi, I. Infante, F. Tarantelli and L. Visscher, *J. Am. Chem. Soc.* 2008, **130**, 1048.

[30] (a) G. Ciancaleoni, L. Biasiolo, G. Bistoni, A. Macchioni, F. Tarantelli, D. Zuccaccia and L. Belpassi, *Chem. Eur. J.* 2015, **21**, 2467; (b) G. Ciancaleoni, N. Scafuri, G. Bistoni, A. Macchioni, F. Tarantelli, D. Zuccaccia and L. Belpassi, *Inorg. Chem.* 2014, **53**, 9907; (c) G. Bistoni, S. Rampino, N. Scafuri, G. Ciancaleoni, D. Zuccaccia, L. Belpassi and F. Tarantelli, *Chem., Sci.*2016, **7**, 1144.

[31] D. Cappelletti, E. Ronca, L. Belpassi, F. Tarantelli and F. Pirani, *Acc. Chem. Res.* 2012, **45**, 1571.

[32] (a) D. Cappelletti, A. Bartocci, F. Grandinetti, S. Falcinelli, L. Belpassi, F. Tarantelli and F. Pirani, *Chem. Eur. J.* 2015, **21**, 6234; (b) A. Bartocci, L. Belpassi, D. Cappelletti, S. Falcinelli, F. Grandinetti, F. Tarantelli and F. Pirani, *J. Chem. Phys.* 2015, **142**, 184304; (c) G. Ciancaleoni, M. Arca, G. F. Caramori, G. Frenking, F. S. S. Schneider and V. Lippolis, *Eur. J. Inorg Chem.*, 2016, **23**, 3804.

[33] G. Ciancaleoni, C. Santi, M. Ragni and A. L. Braga, *Dalton Trans.*, 2015, **44**, 20168.

[34] K. M. Lemishko, G. Bistoni, L. Belpassi, F. Tarantelli, M. M. Montero-Campillo and M. Yáñez (2016), *Charge Transfer in Beryllium Bonds and Cooperativity of Beryllium and Halogen Bonds. A New Perspective* in R. Chauvin et al. (Eds.) *Applications of Topological Methods in Molecular Chemistry* (461-489) Springer Ed., Switzerland.

[35] J. George, V. L. Deringer and R. Dronskowski, *J. Phys. Chem. A*, 2014, **118**, 3193.

36 P. Cardillo, E. Corradi, A. Lunghi, S. V.Meille,M. T. Messina, P.Metrangolo and G.Resnati, *Tetrahedron*, 2000, **56**, 5535.

37 A. Jerschow and N. Müller, *J. Magn. Reson.*, 1997, **125**, 372.

38 R. Mills, *J. Phys. Chem.* 1973, **77**, 685.

39 M. J. Frisch, G. W. T., H. B. Schlegel, G. E. Scuseria, M. A. Robb, J. R. Cheeseman, G.Scalmani, V. Barone, B. Mennucci, G. A. Petersson, H. Nakatsuji, M. Caricato, X. Li, H. P. Hratchian, A. F. Izmaylov, J. Bloino, G. Zheng, J. L. Sonnenberg, M. Hada, M. Ehara, K. Toyota, R. Fukuda, J. Hasegawa, M. Ishida, T. Nakajima, Y. Honda, O. Kitao, H. Nakai, T. Vreven, J. A. Montgomery, Jr., J. E. Peralta, F. Ogliaro, M. Bearpark, J. J. Heyd, E. Brothers, K. N. Kudin, V. N. Staroverov, T. Keith, R. Kobayashi, J. Normand, K. Raghavachari, A. Rendell, J. C. Burant, S. S. Iyengar, J. Tomasi, M. Cossi, N. Rega, J. M. Millam, M. Klene, J. E. Knox, J. B. Cross, V. Bakken, C. Adamo, J. Jaramillo, R. Gomperts, R. E. Stratmann, O. Yazyev, A. J. Austin, R. Cammi, C. Pomelli, J. W. Ochterski, R. L. Martin, K. Morokuma, V. G. Zakrzewski, G. A. Voth, P. Salvador, J. J. Dannenberg, S. Dapprich, A. D. Daniels, O. Farkas, J. B. Foresman, J. V. Ortiz, J. Cioslowski, and D. J. Fox,, *Gaussian 09*, Gaussian, Inc., Wallingford CT, 2013.

40 Y. Zhao and D. Truhlar, *Theor. Chem. Acc.*, 2008, **120**, 215.

41 J. Tomasi, B. Mennucci, R. Cammi, *Chem. Rev.* 2005, **105**, 2999-3094.

42 S. Rampino, VIRT&L-COMM, 2015, **7**, 6.